ELSEVIER

Journal of Power Sources 58 (1996) 99–102

JOURNAL OF POWER SOURCES

Diffusion-limited self-discharge reaction in the Hubble space telescope battery

Joseph P. Fellner [a], Sarwan S. Sandhu [b]

[a] *Wright Laboratory, Wright-Patterson AFB, OH 45433-6563, USA*

[b] *University of Dayton, Dayton, OH 45469-0001, USA*

Received 10 November 1995; accepted 22 December 1995

Abstract

The self-discharge rate of aerospace flight-quality nickel–hydrogen batteries is limited by hydrogen diffusion within the nickel electrode active material. A diffusion-limited reaction model is developed which accounts for the observed self-discharge behavior. Effective hydrogen diffusion coefficients were calculated from the open-circuit self-discharge data on Hubble space telescope flight-qualified nickel–hydrogen cells and ranged from 1.12×10^{-10} cm^2/sec at 25 °C to 7.45×10^{-12} cm^2/sec at 0 °C.

Keywords: Nickel–hydrogen battery; Self-discharge; Diffusion-limited reaction

1. Introduction

Historically, the self-discharge reaction rate of nickel–hydrogen batteries has been proposed to be under kinetic or electrochemical control [1–8]. However, calorimetric measurements on charged nickel electrodes under constant hydrogen pressure indicates that the self-discharge reaction rate is not constant with time [6,9–11]. If the first-order kinetics with respect to hydrogen were controlling the self-discharge, the reaction rate would be constant with time under constant hydrogen pressure. Second-order overall kinetics [4,6], first-order kinetics with respect to hydrogen and β-NiOOH, does not account for the effect of hydrogen diffusion in the solid nickel active material. In a previous electrochemical model [7,8], the effect of non-catalytic chemical reaction and diffusion has also not been accounted for. A simple chemical reaction and diffusion model to explain the self-discharge phenomenon has been previously published [12]. An updated mathematical description of hydrogen diffusion and non-catalytic chemical reaction within the nickel electrode active material to describe the self-discharge of nickel–hydrogen constant volume batteries on open-circuit at various temperatures is presented in this paper. Self-discharge data and their correlation with the simple diffusion-limited reaction model are also presented. The self-discharge data are from the open literature on a constant hydrogen pressure nickel–hydrogen cell and on nickel–hydrogen batteries that are in use on the Hubble Space Telescope [5,6,10].

2. Self-discharge model

To promote rapid oxygen recombination on overcharge, the nickel electrode of the nickel–hydrogen battery operates in an 'electrolyte-starved' condition [13,14]. Therefore, the electrolyte is only present in the micropores of the active material and the macropores of the nickel electrode are free of electrolyte for rapid transport of oxygen produced on overcharge. Assuming that the nickel active material/electrolyte system is a homogeneous mixture, the nickel electrode can be modeled as shown in Fig. 1. Due to the low mass transfer rate, pseudo steady-state thermodynamic equilibrium is

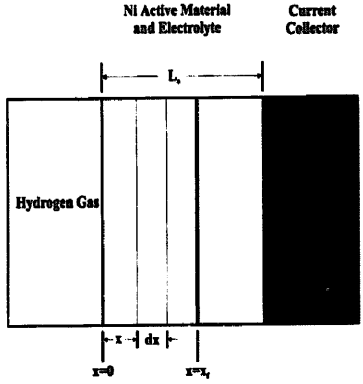

Fig. 1. Schematic diagram of nickel electrode.

Elsevier Science S.A.
PII S0378-7753(96)02329-4

assumed for hydrogen and the concentration of the dissolved gas in the electrolyte at the interface ($x=0$) is represented by Henry's law. Hydrogen is dissolved in the electrolyte and transported in the homogeneous active material/electrolyte mixture and chemically reacts with β-NiOOH to β-Ni(OH)$_2$. This reaction is given by Eq. (1):

$$H_2 + 2\beta\text{-NiOOH} \rightarrow 2\beta\text{-Ni(OH)}_2 \quad (1)$$

A one-dimensional mass balance on hydrogen at $x=x$, (Fig. 1), with constant density, porosity, and diffusivity and with negligible convective transport, results in:

$$\epsilon\frac{\partial C_1}{\partial t} = D_e\frac{\partial^2 C_1}{\partial x^2} - R_1 \quad (2)$$

A mass balance on the nickel oxyhydroxide yields:

$$\frac{\partial C_2}{\partial t} = -R_2 = -2R_1 \quad (3)$$

In dimensionless form, Eqs. (2) and (3) become:

$$\left(\frac{2C_{1,s}\epsilon}{C_{2,0}}\right)\frac{\partial \phi_1}{\partial \tau} = \frac{1}{M^2}\frac{\partial^2 \phi_1}{\partial \xi^2} - R_1^* \quad (4)$$

$$\frac{\partial \phi_2}{\partial \tau} = -R_1^* \quad (5)$$

When $M^2 \ll 1$, the hydrogen diffusion rate is much faster than the kinetic reaction rate and the homogeneous model may be applied. When $M^2 \gg 1$, the kinetic reaction rate is much faster than the diffusion rate and the overall reaction rate is therefore limited by diffusion. When the diffusion and kinetic reaction rates are of the same order of magnitude ($M^2 \sim 1$), then Eqs. (4) and (5) must be simultaneously solved in their full form [15].

From calorimetric measurements on 'starved-electrolyte' nickel electrodes, M^2 appears to be much greater than one [6,9]. Thus, the pseudo steady-state approximation of the hydrogen mass balance leads to:

$$\frac{d^2\phi_1}{d\xi^2} = \frac{d^2 C_1}{dx^2} \cong 0 \quad (6)$$

Integration of Eq. (6) results in the pseudo steady-state approximation of a constant flux with respect to the spatial x-coordinate.

$$N_1 = -D_e\frac{dC_1}{dx} = \text{constant} \quad (7)$$

The instantaneous consumption rate of hydrogen is then given by:

$$-\left(\frac{dn_1}{dt}\right) = S\left(-D_e\frac{dC_1}{dx}\right) \quad (8)$$

Integration of Eq. (6) from $x=0$ to $x=x_f$ and noting that $C_1 = C_{1,s}$ at $x=0$, and $C_1 = 0$ at $x=x_f$, respectively, yields the following equation for the hydrogen concentration distribution.

$$C_1 = C_{1,s}\left(1 - \frac{x}{x_f}\right) \quad (9)$$

Eq. (8) reduces to:

$$\left(-\frac{dn_1}{dt}\right) = \frac{SD_eC_{1,s}}{x_f} \quad (10)$$

The consumption rate of the nickel oxyhydroxide yields:

$$\left(-\frac{dn_2}{dt}\right) = S\rho_2\frac{dx_f}{dt} = 2\left(\frac{dn_1}{dt}\right) \quad (11)$$

Substituting Eq. (10) into Eq. (11) yields:

$$\frac{dx_f}{dt} = 2\frac{D_eC_{1,s}}{\rho_2 x_f} \quad (12)$$

The concentration of hydrogen in the electrolyte at the interface ($x=0$) is given by Henry's law as shown below:

$$P_1 = HC_{1,s} \quad (13)$$

From geometrical considerations, the fractional conversion of β-NiOOH is given by:

$$X_2 = \frac{x_f}{L_a} \quad (14)$$

Substituting for $C_{1,s}$ and x_f from Eqs. (13) and (14), respectively, into Eq. (12) yields:

$$\frac{dX_2}{dt} = \frac{2D_eP_1}{H\rho_2 X_2 L_a^2} \quad (15)$$

For constant hydrogen pressure systems, integration of Eq. (15) leads to the unconverted fraction of nickel oxyhydroxide as shown below:

$$1 - X_2 = 1 - \sqrt{\frac{4D_eP_1t}{H\rho_2 L_a^2}} \quad (16)$$

For a constant hydrogen pressure battery of an initial fully charged capacity of A_0, the capacity with time, A, is then given by:

$$A = A_0(1 - X_2) = A_0\left(1 - \sqrt{\frac{4D_eP_1t}{H\rho_2 L_a^2}}\right) \quad (17)$$

Thus, a plot of remaining capacity versus the square root of open-circuit self-discharge time would yield a straight line.

For constant volume batteries, the fractional conversion of hydrogen and the nickel oxyhydroxide may be defined as:

$$X_1 = X_2 = \frac{P_{1,0} - P_1}{P_{1,0} - P_{1,p}} \quad (18)$$

Thus:

$$\frac{dX_2}{dt} = \left(\frac{1}{P_{1,0} - P_{1,p}}\right)\left(-\frac{dP_1}{dt}\right) \quad (19)$$

Substituting Eqs. (18) and (19) into Eq. (15) yields:

$$\left(\frac{P_{1,0}-P_1}{P_1}\right)\left(-\frac{dP_1}{dt}\right)=\frac{2D_e(P_{1,0}-P_{1,p})^2}{H\rho_2 L_a^2} \quad (20)$$

Integration of Eq. (20) from $t=0$ to t and noting that $P_1=P_{1,0}$ at $t=0$ and $P_1=P_1$ at $t=t$, yields the following equation:

$$\ln\left(\frac{P_1}{P_{1,0}}\right)-\left(\frac{P_1-P_{1,0}}{P_{1,0}}\right)=-\left(\frac{2D_e(P_{1,0}-P_{1,p})^2}{H\rho_2 L_a^2 P_{1,0}}\right)t \quad (21)$$

Thus, a plot of the left-hand side of Eq. (21) versus time should yield a straight line.

Eq. (21) can be further simplified by performing a Taylor expansion of the natural log portion of the left-hand side and retaining the first three terms. Thus:

$$\ln\left(\frac{P_1}{P_{1,0}}\right)=\frac{1}{P_{1,0}}(P_1-P_{1,0})-\frac{1}{2(P_{1,0})^2}(P_1-P_{1,0})^2+\ldots \quad (22)$$

Substituting Eq. (22) into Eq. (21) and simplifying yields:

$$P_1\cong P_{1,0}-\sqrt{\frac{4D_e(P_{1,0}-P_{1,p})^2P_{1,0}}{H\rho_2 L_a^2}}\sqrt{t} \quad (23)$$

Thus, for open-circuit pressures not too far from full charge, the self-discharge behavior of constant-volume batteries can be approximated by Eq. (23). Note that the only variable term on the right-hand side of Eq. (23) is time.

Using Eqs. (18) and (23), the unconverted fraction of β-NiOOH, here defined as the capacity retained (CR), is given by:

$$(1-X_2)=CR\cong 1-\sqrt{\frac{4D_eP_{1,0}}{H\rho_2 L_a^2}}\sqrt{t} \quad (24)$$

Thus, Eq. (24) can be used to approximate the self-discharging behavior of a constant-volume nickel–hydrogen battery on open-circuit starting from a full charge.

3. Validation of the diffusion-limited reaction model

To verify the proposed mathematical model, experimental data from the open literature on self-discharge of nickel–hydrogen batteries were obtained. Data on constant pressure and volume systems were used to generate Fig. 2 and Fig. 3, respectively [5,10].

The set of data for Fig. 2 was obtained from a nickel–hydrogen cell with 31 wt.% KOH in water as the electrolyte, at a constant hydrogen pressure of 150 psig and a temperature of 25 °C. The diffusion-limited reaction model behavior for a constant pressure battery is given by Eq. (17). Using a linear least-squares regression, the model equation was fitted with a coefficient of determination of 0.998.

Data sets for Fig. 3 were obtained from the nickel–hydrogen cells that passed flight qualification testing for the Hubble space telescope. The cells used in these tests were from the same cell lots as the cells that are presently in orbit. To obtain the 0 and 25 °C open-circuit data, the cells were charged at 0 °C. The 20 °C open-circuit data were obtained by charging

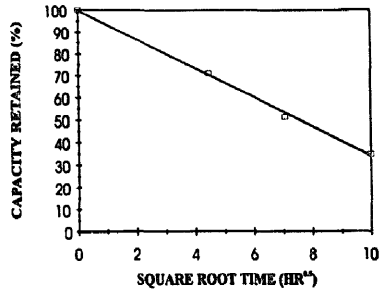

Fig. 2. Nickel–hydrogen cell self-discharge at constant pressure of 150 psig.

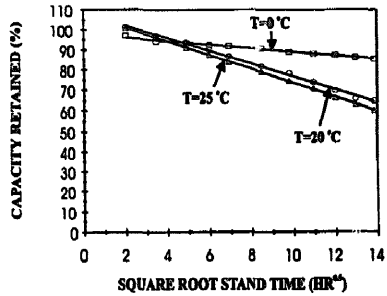

Fig. 3. Hubble space telescope nickel–hydrogen batteries charge retention test.

the cells at 10 °C. Approximation to the diffusion-limited reaction model behavior for a constant volume battery is given by Eq. (24). Using linear least-squares regression, the model equation was fitted to the data with coefficients of determination of 0.994, 0.997, and 0.999 for 0, 20, and 25 °C open-circuit data, respectively.

For a Henry's law constant of 8 918 725 atm cm^3/(g mol) [16], nickel oxyhydroxide molar concentration of 0.042 g mol/cm^3, active material thickness of 5×10^{-4} cm, and a pressure of 11.2 atm, the calculated effective diffusivity from the slope of Fig. 2 is 2.3×10^{-10} cm^2/sec. For a full charge pressure of approximately 68 atm the calculated effective diffusivities from the slopes of Fig. 3 are 1.12×10^{-10}, 9.67×10^{-11}, and 7.45×10^{-12} cm^2/sec for 25, 20, and 0 °C, respectively.

4. Discussion and conclusions

The magnitude of the hydrogen diffusivity calculated from the slopes of Fig. 2 and Fig. 3 is similar to other investigators values who used different techniques [17–19]. Thus, a simple diffusion-limited reaction model adequately explains the self-discharge phenomena in nickel–hydrogen batteries.

The use of cobalt hydroxide in the nickel electrodes for these flight-qualified batteries significantly reduces the amount of oxygen generated near the end of charge, thus neglecting the eff[illegible] of oxygen in the model is justified.

Since the self-discharge rate of nickel–hydrogen batteries is controlled by the diffusion rate of hydrogen in the electrode material, there are several ways to minimize this self-discharge rate. They are (i) increasing the active material thickness on the nickel sinter (ii) decreasing hydrogen operating pressure: (iii) decreasing battery operating temperature, and (iv) using a hydrogen-limited cell design.

5. List of symbols

A	ampere hour capacity
A_0	initial ampere hour capacity
C_1	hydrogen concentration
C_2	β-NiOOH concentration
$C_{1,0}$	initial hydrogen gas concentration
$C_{1,p}$	precharge hydrogen gas concentration
$C_{1,s}$	hydrogen concentration in the electrolyte at $x=0$ (see Fig. 1)
$C_{2,0}$	initial β-NiOOH concentration
CR	capacity retained (fraction unconverted)
D_e	effective diffusivity
H	Henry's law constant
k_1	first order rate constant
L_a	thickness of active material
M^2	$R_1(C_{1,s}; C_{2,0})/(D_eC_{1,s}/L_a^2)$; the Thiele modulus squared which is indicative of the ratio of the maximum reaction rate over a characteristic diffusion rate
n_1	moles of hydrogen
N_1	hydrogen flux rate
n_2	moles of β-NiOOH
P_1	absolute hydrogen pressure corrected for compressibility
$P_{1,0}$	initial corrected hydrogen pressure
$P_{1,p}$	precharge corrected hydrogen pressure
R_1	rate of hydrogen consumption per unit total volume
$R_1{}^*$	$R_1/R_1(C_{1,s}; C_{2,0})$; dimensionless hydrogen consumption rate
R_2	rate of β-NiOOH consumption
S	total (grain + pore) planar surface area of the nickel active material perpendicular to the x-coordinate
t	time
x	distance in nickel active material
x_f	distance in nickel active material where diffusion-limited reaction front occurs
X_2	fractional conversion of β-NiOOH
V_b	battery gas volume

Greek letters

ϵ	β-$Ni(OH)_2$ porosity
ϕ_1	$C_1/C_{1,s}$; dimensionless hydrogen concentration
ϕ_2	$C_2/C_{2,0}$; dimensionless β-NiOOH concentration
ξ	x/L_a; dimensionless distance
ρ_2	β-NiOOH bulk molar density
τ	$2R_1(C_{1,s}; C_{2,0})t/C_{2,0}$; dimensionless time

References

[1] G. Holleck, *Proc. 1977 Goddard Space Flight Center Battery Workshop, NASA-CP-2041, Greenbelt, MD, USA, 1977*, p. 525.

[2] J.F. Stockel, *Proc. 20th Intersociety Energy Conversion Engineering Conf., Miami Beach, FL, USA, 1985*, p. 1.171.

[3] P.F. Ritterman and A.M. King, *Proc. 20th Intersociety Energy Conversion Engineering Conf., Miami Beach, FL, USA, 1985*, p. 1.175.

[4] B.I. Tsenter and A.I. Sluzhevskii, *Zh. Prikl. Khim. (Leningrad), 54* (1981) 2545.

[5] D.E. Nawrocki, J.R. Driscoll, J.D. Armantrout, R.C. Baker and H Waisgras, *Proc. 1992 NASA Aerospace Battery Workshop, NASA-CP-3192, Huntsville, AL, USA, 1992*, p. 293.

[6] A. Visintin, A. Anani, S. Srinivasan, A.J. Appleby and H.S. Lim, *J. Appl. Electrochem., 25* (1995) 833.

[7] Z. Mao and R.E. White, *J. Electrochem Soc., 138* (1991) 3354.

[8] Z. Mao and R.E. White, *J. Electrochem. Soc., 139* (1992) 1282.

[9] A. Visintin, A. Srinivasan, A.J. Appleby and H.S. Lim, *Proc. 6th Ann. Battery Conf Applications and Advances, California State University, Long Beach, CA, USA, 1991.*

[10] Y.J. Kim, A. Visitin, S. Srinivasan and A.J. Appleby, *J. Electrochem. Soc., 139* (1992) 351.

[11] A. Visintin, S. Srinivasan, A.J. Appleby and H.S. Lim, *J. Electrochem. Soc., 139* (1992) 985.

[12] J.P. Fellner, *Proc. 26th Intersociety Energy Conversion Engineering Conf., Boston, MA, USA, 1991*, p. 323.

[13] D. Warnock, S. Gross (ed.), *Proc. Symp. Battery Design and Optimization*, Proc. Vol. 79-1, The Electrochemical Society, Pennington, NJ, USA, 1979, p. 163.

[14] K.M. Abbey and L.H. Thaller, *Pore Size Engineering Applied to Starved Electrochemical Cells and Batteries, NASA-TM-82893*, 1982.

[15] G.F. Froment and K.B. Bischoff, *Chemical Reactor Analysis and Design*, Wiley, New York, 1979. p. 244.

[16] M. Knaster and L. Apelbaum, *Russ. J. Phys. Chem., 38* (1964) 120.

[17] D.M. MacArthur, *J. Electrochem. Soc., 117* (1970) 729.

[18] G.W.D. Briggs, and M. Fleischmann, *Trans. Faraday Soc., 67* (1971) 2397.

[19] G.W.D. Briggs and P.R. Snodin, *Electrochim. Acta, 27* (1982) 565.